

CHARACTERIZING A COHERENT ELECTRON SOURCE EXTRACTED FROM A COLD ATOM TRAP*

Hang Luo, Yanxia Xu, Jie Guo, Peixin Chu, Xi Zhao, Qinghong Zhou, Xiaohong Li, Tao Liu, Kelin Wang, Dept. of Physics, Southwest University of Science and Technology, Mianyang, China

Abstract

In order to generate a fully coherent free electron laser (FEL) within a compact system, one potential approach is to interact a coherent electron bunch with a high power laser operating in the quantum FEL regime. The coherent electron source can be obtained by ionizing the Rydberg atoms in a magneto-optical trap (MOT). The qualities of the electron source will have direct effects on the brightness, coherence, and line width of the free electron laser. A high quality ultra-cold electron source can be obtained by carefully optimizing the extraction electrode structure, the acceleration and focusing system as well as the MOT. Through parameter optimization, a coherent electron source with a temperature lower than 10K is predicted. Details of the optimization and the characteristics of the coherent electron source are reported in this paper.

INTRODUCTION

The planar cathode photoemissive source is simple and stable in performance, and is the most commonly used electron source for time-resolved electron diffraction (TRED) [1], however, the electron source size, effective temperature, the space charge effect, and energy spread [2] factors limit the achievable lateral coherence length [3]; the cutting-edge optoelectronic emission source can be controlled at the sub-femto second time scale [4], which can achieve ultra-short electronic pulse width. It has extremely high coherence and brightness, but the non-uniformity of its initial trajectory and near-field acceleration and the energy spread of electrons lead to the rapid divergence and elongation of the electron beam during propagation [5]. Femtosecond photoemissive sources based on solid cathodes operate well, but lack of coherence [6]. The typical effective field temperature of a conventional field emission or photoemission source is about 5000 K, and the lateral coherence length of an electron pulse has a strong relation with the effective temperature: $L_{\perp} \propto 1/\sqrt{T}$. The lower the temperature, the greater the lateral coherence length. Based on this, we used laser cooling technology to obtain an electron source from a cold atom trap. The electron beam quality will directly affect the brightness, coherence and linewidth of the free electron laser. The electron source transverse temperature obtained by this technology can be as small as 10K or lower, and the atom is very easy to handle, so that coherent electron source can be extracted

from the cold atom. The coherent electron beam can form a very low emittance, coherence temperature. The low emittance of a coherent electron beam results from a high phase space density and a small volume of the coherent electron beam at low temperatures, which is several orders of magnitude lower than conventional electron beam. In addition, the cold electron source can also reach sub-pico-second ultrashort pulse lengths [7]. Thanks to the high coherence and high energy resolution, the cold electron source thus obtained has great applications to various frontier researches.

In order to construct a high-quality ultra-low temperature coherent electron source, a special electrode structure is needed to extract electrons, accelerate and focus. Therefore, we have carried out an optimized design of the electrode structure in the cold atomic trap, and simulated and analyzed the evolution of the three electrode geometries, the position and the influence of the electrode voltage on the electron beam quality.

DEFINITION OF THE QUALITY OF COHERENT ELECTRON

Therefore, our main focus on the coherent electron beam quality factor includes five aspects: energy spread, emittance, electron beam length, beam spot size, and coherent electron beam temperature. Below we give definitions of quality factors:

Energy spread $\frac{\delta}{E}$

Electron beam energy spread has an important impact on the performance of accelerator-based ultrafast scientific devices. The energy spread is closely related to the temperature of the electron, defined as:

$$\frac{\delta}{E} = \frac{\sqrt{\frac{1}{N} \sum_i^N (Ek_i - \langle Ek \rangle)^2}}{\langle Ek \rangle} \times 100\% \quad (1)$$

Emittance

Emittance is the product of the beam size and the opening angle, which is interpreted statistically, that is, using the average of all particles to describe the emittance of the electron beam:

* Work supported by the National Natural Science Foundation of China

Content from this work may be used under the terms of the CC BY 3.0 licence (© 2019). Any distribution of this work must maintain attribution to the author(s), title of the work, publisher, and DOI

$$\varepsilon_{x,rms} = \sqrt{\langle x^2 \rangle \langle x'^2 \rangle - \langle x'x \rangle^2} \quad (2)$$

Electron Beam Length (longitudinal, z-direction)

The length of the particle cluster in the longitudinal direction, which is defined as:

$$length_z = Z_{max} - Z_{min} \quad (3)$$

Beam Waist Size (horizontal, x-y plane)

The beam waist radius of the electron beam is a direct reflection of the electron beam focusing effect, as shown in Fig. 1.

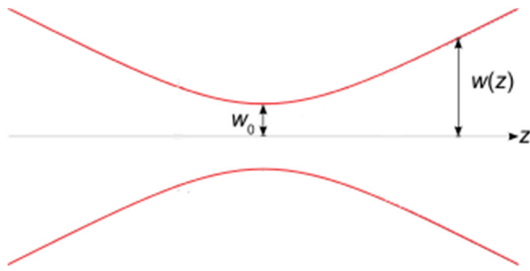


Figure 1: Beam waist $2*w(z)$ as a function of the distance z along the beam. w_0 : beam waist.

Beam width is shown above, we define it as:

$$waist = 2 * \max(\sqrt{x^2 + y^2}) \quad (4)$$

$waist$ is the beam spot size, and x and y are the positions of the electrons in the coordinate system.

Coherent Electron Beam Temperature

We use the effective temperature of the electron under classical conditions. In this design, the electrons have no freedom of rotation and vibration, and we only consider the direction of coherent electron beam transmission, so the coherent electron beam temperature is defined as:

$$T = \frac{mv_{rms}^2}{k} \quad (5)$$

MODELING

The electron beam quality is directly affected by the electric field distribution. We change the electric field distribution by changing the electrode structure and position. In the model, in order to find the appropriate electrode structure and related parameters, we can simulate the electron beam quality. According to the initial requirements, we have established two parallel equal-large electrode plates with aperture, length and spacing $r1 \times L1 \times d1$, $r2 \times L2 \times d2$ respectively. Place a sphere with a spherical radius $r1$ as an electron cluster at a suitable position.

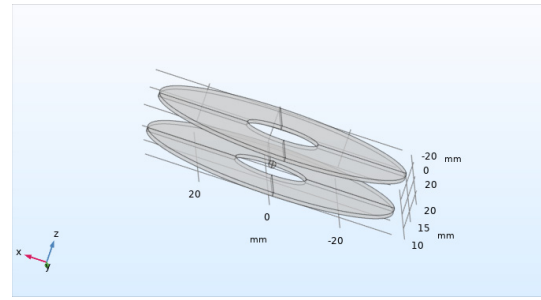


Figure 2: Two electrode plate geometry models.

According to the optimized design, the four pieces design is chosen as the parallel electrode plates. First, in order to make the electrons in the negative electric field, we give priority to the field shielding problem. The first and second boards $V1=V2=-20KV$ are negative voltages, and the two boards have the same voltage, so as to reduce the leakage through the electrode holes. Comparing their potential maps in Fig. 3(c) and (d), we can easily see that. The influence of the positive electric field between $V1$ and the cavity on the electron group; the third plate voltage $V3=-5KV$, which is a variable negative voltage, the purpose is to weaken the complex field leakage at the aperture, and the second is to reduce the kinetic energy loss by adjusting, as shown in Fig. 3(a) to (e). It is the position where the coherence temperature can be controlled when the electronic output is minimum, as shown in Fig. 3(b); the last board is connected to $V4=0V$ for field shielding; the external cavity is grounded to avoid danger.

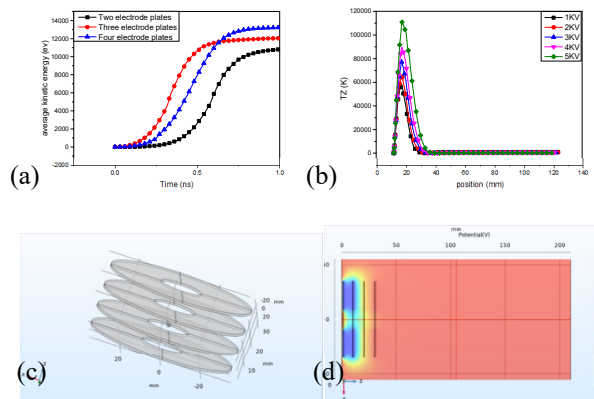


Figure 3: (a) Average kinetic energy obtained by different numbers of parallel plates; (b) The relationship between the coherent electron temperature and the electronic position of the third electrode plate at different voltages; (c) Four electrode plate geometry models; (d) potential distribution map.

SIMULATION RESULTS

In the parallel plate electrode model, when the voltages across the parallel plates are the same, the electric field quality is changed by changing the electric field distribution in the cavity by the displacement operation of the parallel plates. At this time, the electrode voltage $V1=V2=-$

20KV, V3=5KV, the hole radius $r_1=r_2=r_3=r_4=10\text{mm}$, the length $L_1=L_2=L_3=L_4=60\text{mm}$, the distance between plates $d_1=d_2=d_3=10\text{mm}$, currently we show the data obtained when the electrode is displaced. The electron beam quality changes with the electric field distribution. The results are shown in different spatial positions as shown in Fig. 4. It shows a set of optimized results.

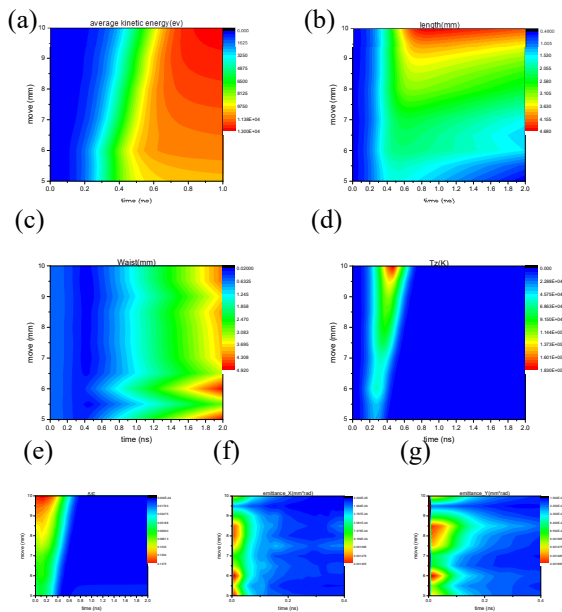


Figure 4: The x-axis is time, y-axis is the moving distance of the electrode plate, the representative color value to: (a) average kinetic energy; (b) electron beam length; (c) electron beam waist; (d) Coherent electron beam temperature; (e) δ / E ; (f) emittance_X; (g) emittance_Y.

When the electron beam moves to the 0.4m position, the electron beam energy spread $\frac{\delta}{E} < 0.032\%$ as shown in Fig. 4(e); At this time, in the direction of electron beam transmission, the coherent electron beam temperature is controlled within 10K, coherent electron beam temperature as shown in Fig. 4(d), which satisfies our initial experimental requirements, and is consistent with M.W. van Mourik and W.J. Engelen in 2014 for ultra-fast electron diffraction experiments at 10K; The electron emittance in the X and Y direction is all $\varepsilon < 0.2 \text{ mm.mrad}$, as shown in Fig. 4(c) and (d); when the electron beam is at this position, the beam length is $\text{length}_z < 3.6\text{mm}$ as shown in Fig. 4(b); The beam waist size is around 1.4 mm, as shown in Fig. 4(c).

DISCUSSIONS

In the continuous simulation analysis, we found that there are at least two problems to be dealt with urgently. First, the large aperture and the spatial position of the electrons cause the kinetic energy loss of the electrons to be excessively large. as shown in Fig. 5(a), (b); Second, we

minimize the positive electric field to the electrons. The influence of the regiment is far from enough to shield, which is also the root cause of the loss of kinetic energy obtained by our electronics. At present, we still need to upgrade the structure and optimize the parameters in order to maintain the quality of other electron beams in the case of kinetic energy loss.

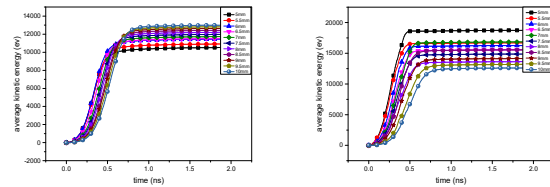


Figure 5: (a) Different moving distances of the electrode plates, the average kinetic energy changes with time. (b) Different hole radii of the electrode plate, the average kinetic energy changes with time.

CONCLUSION

In summary, the more complex the model, the more uncontrollable variables are generated. At present, we can determine the optimization research object as the parallel plate geometry model. The electron beam energy spread $\frac{\delta}{E} < 0.032\%$, and the coherent electron beam temperature is within 10K. The electron emittance in the X and Y direction is all $\varepsilon < 0.2 \text{ mm.mrad}$, and the beam length $\text{length}_z < 3.6 \text{ mm}$. The beam waist size is about 1.4 mm. All of the above are the design of the first stage electrode in the cavity. We will add the electrode to the electron beam for secondary regulation outside the cavity.

REFERENCES

- [1] M.S. Robinson *et al.*, "A compact electron gun for time-resolved electron diffraction", *Review of Scientific Instruments*, 86(1), 013109 (2015). doi:10.1063/1.4905335
- [2] G. Sciaini *et al.*, "Femtosecond electron diffraction: heralding the era of atomically resolved dynamics", *Reports on Progress in Physics*, 74(9), 096101 (2011). doi:10.1088/0034-4885/74/9/096101
- [3] T. van Oudheusden *et al.*, "Electron source concept for single-shot sub-100 fs electron diffraction in the 100 keV range", *Journal of Applied Physics*, 102(9), 93501-0 (2007). doi:10.1063/1.2801027
- [4] K. Krüger *et al.*, "Attosecond control of electrons emitted from a nanoscale metal tip", *Nature*, 475 (7354), 78-81 (2011). doi:10.1038/nature10196
- [5] A. Paarmann *et al.*, "Coherent femtosecond low-energy single-electron pulses for time-resolved diffraction and imaging: A numerical study", *Journal of Applied Physics*, 112(11), 113109 (2012). doi:10.1063/1.4768204.
- [6] S.B. van der Geer *et al.*, "Ultracold Electron Source for Single-Shot, Ultrafast Electron Diffraction", *Microscopy and*

Microanalysis, 15(04), 282-289 (2009).
doi:10.1017/S143192760909076X

- [7] O.J. Luiten *et al.*, “Ultracold Electron Sources”, *International Journal of Modern Physics A*, 22(22), 3882-3897 (2007). doi:10.1142/S0217751X07037494

Content from this work may be used under the terms of the CC BY 3.0 licence (© 2019). Any distribution of this work must maintain attribution to the author(s), title of the work, publisher, and DOI